Physics Letters A ••• (••••) •••–•••

Contents lists available at ScienceDirect

Physics Letters A

www.elsevier.com/locate/pla

Negative differential resistance and rectification effects in zigzag graphene nanoribbon heterojunctions: Induced by edge oxidation and symmetry concept

Maryam Nazirfakhr *, Ali Shahhoseini *

Department of Electrical, Biomedical, and Mechatronics Engineering, Qazvin Branch, Islamic Azad University, Qazvin, 3419915195, Iran

ARTICLE INFO

Article history:
Received 15 September 2017
Received in revised form 13 December 2017
Accepted 3 January 2018
Available online xxxx
Communicated by R. Wu

Keywords:
Zigzag graphene nanoribbon
Heterostructure
Electronic transport properties
Rectifying performance
Negative differential resistance

ABSTRACT

By applying non-equilibrium Green's functions (NEGF) in combination with tight-binding (TB) model, we investigate and compare the electronic transport properties of H-terminated zigzag graphene nanoribbon (H/ZGNR) and O-terminated ZGNR/H-terminated ZGNR (O/ZGNR–H/ZGNR) heterostructure under finite bias. Moreover, the effect of width and symmetry on the electronic transport properties of both models is also considered. The results reveal that asymmetric H/ZGNRs have linear I–V characteristics in whole bias range, but symmetric H-ZGNRs show negative differential resistance (NDR) behavior which is inversely proportional to the width of the H/ZGNR. It is also shown that the I–V characteristic of O/ZGNR–H/ZGNR heterostructure shows a rectification effect, whether the geometrical structure is symmetric or asymmetric. The fewer the number of zigzag chains, the bigger the rectification ratio. It should be mentioned that, the rectification ratios of symmetric heterostructures are much bigger than asymmetric one. Transmission spectrum, density of states (DOS), molecular projected self-consistent Hamiltonian (MPSH) and molecular eigenstates are analyzed subsequently to understand the electronic transport properties of these ZGNR devices. Our findings could be used in developing nanoscale rectifiers and NDR devices.

1. Introduction

Graphene, as a two-dimensional (2D) honeycomb carbon structure, has attracted tremendous interest after becoming experimentally accessible with techniques such as mechanical exfoliation [1–3] and chemical-vapor deposition (CVD) [4,5]. Graphene is expected to have extensive applications in the future nanoelectronic devices due to its unique electronic transport properties such as high electron mobility, high thermal conductivity, etc. [6–9]. In order to build nanoelectronic devices, zero-gap graphene sheets usually need to be cut into GNRs [10,11]. According to their edge configurations, GNRs are classified into two main categories: ZGNRs and armchair graphene nanoribbons (AGNRs). ZGNRs are metallic because of the degeneration of the two edge states at the Fermi level, while AGNRs can either be metallic or semiconducting with different energy gaps depending upon the width of the ribbons [12–14]. In recent years, progress in experimental fabrication technology has made it possible to design and build nanoscale devices in which many interesting physical features have been observed, such as rectification [15–22], NDR [22–26], switching behavior [27–30], field-effect characteristics [31–33], spin filtering [34,35], etc.

The idea of molecular rectification was proposed by Aviram and Ratner [15] in 1974 and since then it has been the subject of numerous experimental and theoretical investigations [15–22]. In [17] J. Zeng et al. have studied the electronic transport properties of mono hydrogenated and di-hydrogenated ZGNR heterojunctions under finite bias voltages. They have reported perfect spin filtering effect and rectifying behavior. Wang et al. [18] have demonstrated a ballistic rectifying behavior by applying an external gate voltage to an AGNR-ZGNR-AGNR heterostructure. Can Cao et al. [19], have investigated ZGNR heterojunctions. They found a remarkable rectifying behavior by adjusting the edge hydrogenation. Yipeng An et al. [22], have studied the Step-like ZGNRs with different step widths. The results reveal that these step-like ZGNR nanojunctions present valuable rectification effects. Zhao et al. [24] observed noticeable rectifying and NDR behaviors in nitrogen-doped AGNRs. Both behaviors were strongly correlated with the doping position.

* Corresponding authors.
E-mail addresses: MaryamNazirfakhr@yahoo.com (M. Nazirfakhr), Shahhoseini@qiau.ac.ir (A. Shahhoseini).

https://doi.org/10.1016/j.physleta.2018.01.001
0375-9601/

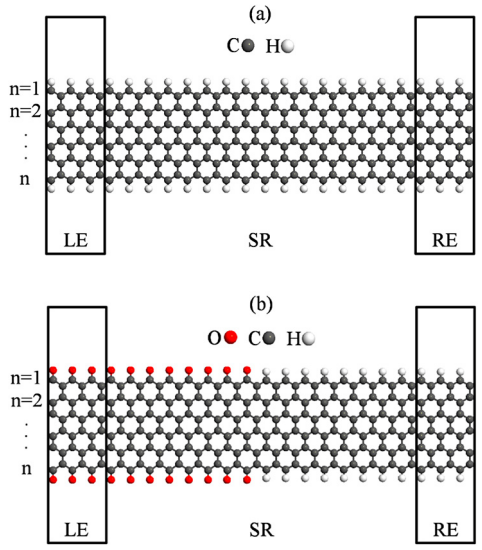

Fig. 1. The optimized geometry of the device. (a) H/ZGNR and (b) H/ZGNR-O/ZGNR heterostructures. n is an integer which denotes the number of zigzag chains. Even n refers to a symmetric ZGNR, while odd n expresses an asymmetric one. (A/B)1, (A/B)2, (A/B)3 and (A/B)4 correspond to $n = 3$, 4, 5 and 6, respectively.

Although, molecular rectifiers have been studied extensively, but the corresponding studies are still inadequate and not applicable to industrialized production. So, in order to design and produce high-performance molecular rectifiers, further researches are needed. Among chemical candidates for edge passivation, oxygen draws further attention due to its universal existence and comparable radius as carbon atoms. In this paper, we investigate and compare the electronic transport properties of H/ZGNR and H/ZGNR-O/ZGNR heterostructure under finite bias (−1 V to +1 V). Moreover, we study the effects of symmetry and width of ZGNR on the electronic transport properties of these two models.

This paper is organized as follows: In Section 2, we present our model and the simulation method. In section 3 the results are discussed. Finally a conclusion of our results is given in Section 4.

2. Model and simulation

Fig. 1 displays two structures (A, B) as a representative for all our models. In A group models (A1–A4) the edge carbon atoms of the ZGNR are terminated by hydrogen (Fig. 1(a)), while B group models (B1–B4) are heterostructures in which the edge carbon atoms of the left half of the ZGNR are oxygen terminated and the ones of the right half are terminated by hydrogen (Fig. 1(b)). The systems are divided into three main regions: left electrode (LE), right electrode (RE) and the central scattering region (SR). In both A and B models, each electrode and the central scattering region are described by supercells with 3 and 16 repeated carbon unit cells along the transport direction, respectively. In order to study the effects of width and symmetry of the ZGNR on the electronic transport properties, we consider $n$as an integer which denotes the number of zigzag chains. Even n refers to a symmetric ZGNR, while odd n expresses an asymmetric one. (A/B)1, (A/B)2, (A/B)3 and (A/B)4 correspond to $n = 3$, 4, 5 and 6, respectively.

The electronic transport properties are studied, using the SCC-DFTB combined with NEGF formalism. All the calculations are performed in DFTB+ package [36]. mio parameters set is used for TB calculations. The current is calculated by Landauer–Büttiker formula:

$$I = \frac{2e}{h}\int_{\mu_L}^{\mu_R} T(E, V_b)\big[f(E, \mu_L) - f(E, \mu_R)\big]dE$$

Where h is Planck's constant, e is the electron charge. $\mu_R = E_f + |e|(V/2)$ and $\mu_L = E_f - |e|(V/2)$ are the chemical potentials of the right and left electrodes, $T(E, V_b)$ represents the transmission coefficient, V_b is the applied bias voltage across the electrodes and $f(E, \mu)$ is the Fermi–Dirac distribution.

The Monkhorst–Pack k-points grid is set $1 \times 1 \times 100$ to sample the Brillouin zone of the electrodes. The mesh cut-off is chosen to be 150 Ry. Geometry optimization is performed until the force is less than 0.05 eV/Å. The convergence criteria for Hamiltonian and the electron density is 10^{-5}. The electron temperature is set to 300 K in the transport calculations. Initially, we minimize the total energy of the nanoribbons, and then by applying bias voltage along it, the current is computed. The applied bias voltage is increased from −1 V to +1 V in steps of 0.1 V. The vacuum pad along x and y directions are 20 and 40 Å, respectively.

3. Results and discussions

In Fig. 2, the self-consistently calculated current-voltage (I–V) characteristics for all discussed molecular configurations, are presented at the bias range from −1 V to 1 V in steps of 0.1 V. The I–V characteristics of symmetric and asymmetric H/ZGNR (A1–A4) are shown in Fig. 2(a) and (b). From Fig. 2(a) it can be found that under positive and negative bias voltages, the currents of asymmetric A1 and A3 models increase quickly and almost linearly with the increase of applied bias voltage. Moreover, we see that increasing the width of H/ZHNR has almost no effect on the I–V characteristics, and an identical symmetric behavior is observed in A1 and A3. Fig. 2(b) depicts the I–V curves of symmetric A2 and A4 models, which are slightly different but both of them show a symmetric behavior in total bias range. The I–V curves of recent models show a linear behavior up to 0.1 V, but when the applied bias voltage exceeds 0.1 V, they oscillate and NDR behavior is observed. It is clear that by increasing the width of the ribbon, the peak-to-valley ratio which is an important quantity to measure the NDR behavior is diminished. Comparing Fig. 2(a) and (b), it can be found that asymmetric and symmetric H/ZGNRs have symmetric but different transport characteristics. Furthermore, it is obvious that the current of asymmetric H/ZGNR is much bigger than the current of symmetric H/ZGNR. For instance, at 0.6 V, the currents of A1 to A4 are 46.34, 2.77, 46.12 and 4.72 μA, respectively.

The I–V characteristics of symmetric and asymmetric H/ZGNR-O/ZGNR heterostructures (B1–B4) are shown in Fig. 2(c) and (d). As you see, the I–V curves are asymmetric and a rectification effect is observed for B1 to B4. Comparing B1 and B3 (Fig. 2(c)), it is found that by increasing the number of zigzag chains from 3 to 5, the current is increased in whole bias range, but $I(-V)$ increment is a bit more than $I(+V)$. The biggest rectification ratio for B1 and B3 is seen at 1 V, which is 3.53 and 2.09, respectively. As you see, the rectification ratio is reduced about 1.44. Fig. 2(d) depicts the I–V characteristics of B2 and B4. It is observed that, by increasing the number of zigzag chains from 4 to 6, the current is increased in whole bias range (pay attention to the inset of Fig. 2(d)). It should be noted that the increment of I under positive voltages is more than the increment of I under negative voltages. The best rectification ratio for B2 and B4 is $R_{B2} = 993 \times 10^6$ (at 0.9 V) and $R_{B4} = 173$ (at 0.7 V), respectively.

Generally, we see that the rectification ratio in symmetric O/ZGNR–H/ZGNR heterostructures is strongly correlated with the width of ZGNR, while which is not the case for asymmetric ones. Comparing: (1) A1/A3 with B1/B3 it is found that substituting hydrogen atoms at the edge of the ZGNR with oxygen, nearly has no effect on $I(+V)$, but it reduces $I(-V)$. (2) A2/A4 with B2/B4 it is observed that by applying this change, $I(+V)$ is increased, while $I(-V)$ is decreased. Generally it can be found that, by choosing a

Please cite this article in press as: M. Nazirfakhr, A. Shahhoseini, Negative differential resistance and rectification effects in zigzag graphene nanoribbon heterojunctions: Induced by edge oxidation and symmetry concept, Phys. Lett. A (2018), https://doi.org/10.1016/j.physleta.2018.01.001